



**HAL**  
open science

## Effect of the presence of pyrite traces on silver behavior in natural porous media

Delphine Charrière, Manuel de A. Hernández Cortázar, Philippe Behra

► **To cite this version:**

Delphine Charrière, Manuel de A. Hernández Cortázar, Philippe Behra. Effect of the presence of pyrite traces on silver behavior in natural porous media. *Journal of Colloid and Interface Science*, 2015, 446, pp.379-385. 10.1016/j.jcis.2014.12.050 . hal-02531431

**HAL Id: hal-02531431**

**<https://hal.science/hal-02531431>**

Submitted on 3 Apr 2020

**HAL** is a multi-disciplinary open access archive for the deposit and dissemination of scientific research documents, whether they are published or not. The documents may come from teaching and research institutions in France or abroad, or from public or private research centers.

L'archive ouverte pluridisciplinaire **HAL**, est destinée au dépôt et à la diffusion de documents scientifiques de niveau recherche, publiés ou non, émanant des établissements d'enseignement et de recherche français ou étrangers, des laboratoires publics ou privés.





## Open Archive Toulouse Archive Ouverte (OATAO)

OATAO is an open access repository that collects the work of Toulouse researchers and makes it freely available over the web where possible

This is an author's version published in: <http://oatao.univ-toulouse.fr/25435>

**Official URL:** <https://doi.org/10.1016/j.jcis.2014.12.050>

**To cite this version:**

Charrière, Delphine  and Hernández Cortázar, Manuel de A. and Behra, Philippe  *Effect of the presence of pyrite traces on silver behavior in natural porous media.* (2015) *Journal of Colloid and Interface Science*, 446. 379-385. ISSN 0021-9797

Any correspondence concerning this service should be sent to the repository administrator: [tech-oatao@listes-diff.inp-toulouse.fr](mailto:tech-oatao@listes-diff.inp-toulouse.fr)

# Effect of the presence of pyrite traces on silver behavior in natural porous media

Delphine Charrière<sup>a,b</sup>, Manuel de A. Hernández Cortázar<sup>c</sup>, Philippe Behra<sup>a,b,\*</sup>

<sup>a</sup> Université de Toulouse; INPT, LCA (Laboratoire de Chimie Agroindustrielle), UMR 1010, ENSIACET, 4, Allée Emile Monso, CS 44362, F-31030 Toulouse Cedex, France

<sup>b</sup> INRA, LCA (Laboratoire de Chimie Agroindustrielle), F-31030 Toulouse, France

<sup>c</sup> CMP+L (Centro Mexicano para la Producción más Limpia Instituto Politecnico Nacional), Av. Acueducto S/N, col. Barrio la Laguna, Ticoman, 07340 México, D. F., Mexico

## ARTICLE INFO

### Keywords:

Silver  
Speciation  
Sorption  
Quartz sand  
Pyrite  
Langmuir-type model  
Reduction  
Colloids

## ABSTRACT

In order to better understand the fate of the toxic element Ag(I), sorption of Ag(I) was studied from batch experiments, at different pHs (2–8) and at 298 K. A pure quartz sand (99.999% SiO<sub>2</sub>) and “natural” quartz sand (99% SiO<sub>2</sub>, and traces of Fe, Al, Mn (hydr)oxides, of clays and of pyrite) were used as sorbents. The Ag(I) sorption behavior depends strongly on pH with isotherm shapes characteristic of Langmuir type relationship for initial Ag concentration [Ag(I)], range between  $5.0 \times 10^{-7}$  and  $1.0 \times 10^{-3}$  M. Even if the Ag(I) sorption capacity on pure quartz sand is very low compared to the natural quartz sands, its affinity is rather high. From speciation calculations, several sites were proposed: at pH, 4, 6 and 8, the first surface site is assumed to be due to iron (hydr)oxides while the second surface site is attributed to silanols. At pH, 2, sorption of Ag(I) was assumed to be on two surface sites of iron (hydr)oxides and a third surface site on silanol groups. Even if the sand is mainly composed of silica, the trace minerals play an important role in sorption capacity compared to silica. The conditional surface complexation constants of Ag(I) depend on pH. On the other hand, it is shown that the Ag speciation depends strongly on the history of “natural” quartz sand due to initial applied treatment, little rinsing or longer washing. In the presence of low amount of pyrite, strong complexes between Ag(I) and sulfur compounds such as thiosulfates due to oxidative dissolution of pyrite are formed what decreases Ag sorption capability. SEM EDS analyses highlighted the surface complexation precipitation of Ag<sub>2</sub>S and Ag(0) colloids which confirmed the important role of pyrite on Ag(I) speciation.

## 1. Introduction

Interactions of heavy metals at liquid liquid and liquid solid interfaces have been largely studying by the scientific community due to their role in the understanding of environmental pollution owing to the various human activities: metallurgy, dentistry, chemistry, nuclear industry, paint and batteries, and agricultural habits such as the use of fertilizers, fungicides and other pesticides. To prevent migration of heavy metal pollutants in wastewater, contaminated soil and solid waste, knowledge of mechanisms controlling transport and transfer of metals which occurs at the solid liquid interface is thus a prerequisite. The possible mechanisms are numerous: precipitation, dissolution, sorption, complexation, oxidoreduction, etc. Silver is considered as a toxic metal

either if present in cationic form, Ag(I), or as nanoparticles, mainly Ag(0) [1–3]. Anthropogenic activities (mining, steel mills, cement plants, burning fossil fuel, nuclear, biocides, etc.) have been among the main sources of Ag(I) in natural systems [1–5]. Nowadays its biocide effects when used as nanoparticles are considered as very strong and explained why Ag is very often present in its colloidal forms in the environment [1]. The maximum silver concentration in drinking water is recommended at  $50 \mu\text{g L}^{-1}$  by the World Health Organization (1975) and limited at  $10 \mu\text{g L}^{-1}$  in the European Union (98/83/CE). Silver is also included in the US EPA list of priority toxic pollutants. Thus, to avoid pollution, understanding the phenomena of sorption is essential to predict the speciation of Ag(I) and Ag nanoparticles in environmental system and matrix [1].

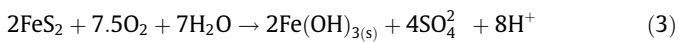
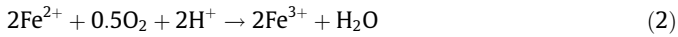
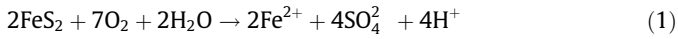
Ag(I) can form complexes with ligands present in the environment. It may, in the case of Ag(I), form stable complexes with ammonia, cyanide, thiosulfate, and halide. Silver sulfide, Ag<sub>2</sub>S, is one of the most insoluble silver salts. However, the solubility of

\* Corresponding author at: INPT, INRA, LCA (Laboratoire de Chimie Agroindustrielle), F-31030 Toulouse, France.

E-mail address: philippe.behra@ensiacet.fr (P. Behra).

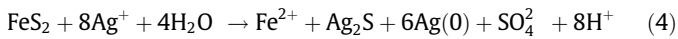
the salt can change with the presence of organic or inorganic ligands which form complexes depending on pH, ionic strength, redox conditions, etc. Few studies have reported on Ag(I) sorption on different natural minerals [6–9].

For example, the surface of pyrite is known for its properties of adsorption and retention of precious metals such as gold, silver, platinum and also mercury [10]. Moreover, the oxidative dissolution of pyrite releases aqueous  $\text{SO}_4^{2-}$ , Fe(II) and Fe(III) in acidic medium and  $\text{SO}_4^{2-}$  and iron (hydr)oxides  $\text{FeOOH}_{(s)}$  in basic medium [11,12]:

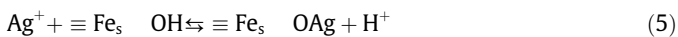


Rate law of pyrite oxidation has been reported by Williamson and Rimstidt [13], taking into account the  $\text{O}_2$  and  $\text{H}^+$  molalities. Recently, Gartman and Luther III [14] have shown that the oxidation rate of sub micron pyrite in seawater is first order with respect to both  $\text{O}_2$  and pyrite concentration.

Scaini et al. [6] have worked on the interaction of Ag(I) ( $[\text{Ag}(\text{I})] = 10^{-4} \text{ M}$ ) with pyrite, at pH 3. Analyses of the solution after reaction have displayed measurable amounts of  $\text{Fe}^{2+}$ . According to their results, the presence of  $\text{Ag}_2\text{S}$  and the deposition of metallic silver (XPS and SEM analysis) have been detected on the surface of pyrite. In conclusion they have proposed the following mechanism [6]:



Ravikumar and Fuerstenau [7] have studied the Ag(I) sorption on cryptomelane, a manganese oxide. Sorption depends on surface chemistry of oxide and chemical composition of solution (e.g. pH). They have proposed an ion exchange reaction mechanism between Ag(I) and potassium [7]. In addition, Dzombak and Morel [8] have estimated many surface complexation constants of several metals with hydrous ferric oxide (HFO). They have concluded that the adsorption capacity of Ag(I) is higher at basic pH and that sorption is controlled by formation of monodentate surface complex. For the strong surface sites (s), Ag sorption is described by the following surface complexation reaction:



the surface complexation constant being estimated at  $10^{1.72}$ , for  $0.1 \text{ mM } [\text{Ag}(\text{I})]$  (for the weak surface site, the surface complexation constant is  $10^{5.3}$ ).

Moreover they have concluded that the behavior of Ag(I) could be controlled by a mechanism of complexation precipitation at high pH and at Ag(I) concentration below  $600 \mu\text{M}$  [8]. Jacobson et al. [9] have studied the Ag(I) sorption on various soils with different organic matter content and composition. In their conclusion they have stated that even if Ag(I) sorption is dominated by organic matter, illitic clays play an important role in retaining Ag(I).

The present work focused on the sorption of Ag(I) on three materials: a pure quartz sand, a washed and rinsed natural quartz sands. The raw natural quartz sand was shown to have small amounts of pyrite, clays and (hydr)oxides of Fe, Mn and Al. The objective was to understand the behavior of Ag(I) in the presence of different sands by identifying possible sorption mechanisms and estimating surface parameters. The sorption isotherm experiments of Ag(I) performed at 4 initial pHs (2–8) were analyzed by XPS and modeled according to Langmuir type isotherms with 1, 2 or 3 sites. In addition, to highlight an area of precipitation, experiments with higher concentrations of Ag(I) ( $10^{-2} \text{ M}$ ) at pH 6 were

performed. The products of reactions between sand minerals and Ag(I) were confirmed by SEM EDS analysis.

## 2. Theories

### 2.1. Langmuir type relationship

The Langmuir model [15] has been developed to study the equilibrium at gas–solid interface. Owing to similar shaped isotherms, this model has been extended for probing the sorption phenomenon at liquid–solid interface [16]. Some mathematic relationships have been adopted for fitting the experimental data. In this case the solution species, A, can be adsorbed on surface sites of a solid adsorbent  $\equiv\text{S}$ , with a 1:1 stoichiometry and  $\equiv\text{SA}$ , the adsorbate, present at the surface [17]:



The concentrations of  $\equiv\text{S}$  and  $\equiv\text{SA}$  are in  $\text{mol m}^{-2}$ . The equivalent of maximum surface site concentration in experimental conditions ( $\text{mol m}^{-2}$ ) is:

$$\Gamma_{\text{max}} = \Gamma_{\equiv\text{S}} + \Gamma_{\equiv\text{SA}} \quad (7)$$

For two or more surface sites,  $\Gamma_1, \Gamma_2, \dots, \Gamma_n$ , which correspond to different site affinities, the relationship between the adsorbed and the aqueous concentrations of A can be calculated at equilibrium according to the Langmuir type model [17]:

$$\Gamma = \sum_{i=1}^n \Gamma_{\text{max},i} \frac{K_{\text{ads},i} [\text{A}]_{\text{aq}}}{1 + K_{\text{ads},i} [\text{A}]_{\text{aq}}} \quad (8)$$

where  $K_{\text{ads},i}$  is the Langmuir type constant ( $\text{L mol}^{-1}$ ),  $[\text{A}]_{\text{aq}}$  is the total aqueous concentration of A ( $\text{mol L}^{-1}$ ),  $\Gamma$  is the total sorbed concentration of Ag(I) ( $\text{mol m}^{-2}$ ), and  $\Gamma_{\text{max},i}$  is the equivalent of maximum surface site concentration in experimental conditions ( $\text{mol m}^{-2}$ ). The parameters,  $\Gamma_{\text{max},i}$  and  $K_{\text{ads},i}$  can be directly estimated, from experimental data with specific software, such as Origin spreadsheet.

The relationship between Langmuir type model and surface complexation is described in more details in the [Supporting information](#).

### 2.2. Speciation software: MICROQL

The software MICROQL [18,19] was used for speciation calculation of the adsorption of a given solute on mineral surfaces. The reactions and mass balances which are necessary for calculation are reported as a Tableau in [Table S1](#) [20] (see the [Supporting information](#) for more detail about surface acidity and aqueous speciation theories).

## 3. Materials and methods

### 3.1. Sorbent materials

Three sorbent materials were used: (i) a pure quartz sand, (ii) a natural quartz sand washed in a column (treatment I) and (iii) the same natural quartz sand rinsed with pure water (treatment II).

#### 3.1.1. Pure quartz sand

This material was purchased from the “Quartz & Silica Company” in Nemours (Seine et Marne, France). It was produced by heating silica at  $1000^\circ\text{C}$  and treating with hydrofluoric acid and recrystallizing for purification. According to the company, and to XPS surface analyses, the pure quartz sand is composed of 99.999%  $\text{SiO}_2$  at its surface [21]. The specific surface area is rather low,

about  $0.033 \text{ m}^2 \text{ g}^{-1}$  ( $\text{N}_2/\text{He}$ , 77 K, BET, QSurfM1, Thermo Finnigan), and the range of grain size is between 100 and  $620 \mu\text{m}$  [22].

### 3.1.2. Natural quartz sand

Natural quartz sand was provided by "Quartz d'Alsace" Company in Kaltenhouse (North of Strasbourg, France). This sand was a natural product which was washed, sieved, and dried at  $105^\circ\text{C}$  by the manufacturer. The mineral composition of sand was studied by Behra [23,24] and contains 99%  $\text{SiO}_2$ , 1% potassic feldspars,  $\sim 0.1\%$  clays (among: kaolinite and illite) and traces of Fe, Mn and Al (hydr)oxides. Some pyrite in the natural quartz sand is also present in cubic and globular forms (Fig. S1a and S1b). From size analysis, it can be shown that the surface and grain size of the sand are very heterogeneous and porous. The grain size median diameter ( $d_{50}$ ) and characteristic diameter ( $d_{10}$ ) are approximately  $650 \mu\text{m}$  and  $430 \mu\text{m}$ , respectively [21]. The specific surface area is rather high, about  $0.16 \text{ m}^2 \text{ g}^{-1}$  (Kr, 77 K, BET) [21] with respect to the grain size distribution. The point of zero charge is about pH 6, showing the presence of metal (hydr)oxides at surface grains [25].

### 3.1.3. Sand treatment

For sorption experiments, two types of treatment were performed. For the primary experiments and for initial pH<sub>i</sub> 2, 4, 6 and 8, the sand was washed with demineralized water in a column (treatment I). This treatment lasted approximately 20 days to obtain a constant value of pH (Knick 765 calimatic, Orion Ross combined glass electrode 8102) and conductivity (Knick 703). For other experiments performed at initial pH<sub>i</sub> 6 and at a high concentration of Ag(I), the sand was rinsed with demineralized water for a brief period ( $\sim 10$  min) (treatment II). This treatment resulted in few significant changes of surface. The two sands were then dried in an oven at  $40^\circ\text{C}$  for 4 h and kept at room temperature ( $20^\circ\text{C}$ ) prior to use in sorption experiments.

According to the composition, this natural quartz sand represents, at a small scale, a sample of aquifer material. This sand was used to characterize the behavior of other pollutants, notably Hg [23,25], TBT [21,25,26], Cd, Pb [27] and As [28]. Kinetic and isotherm experiments of Ag(I) sorption on natural quartz sand (treatment I) have been ever presented by Hernandez and Behra [29] but without discussion of results. In these previous studies, minerals of pyrite have never been highlighted and could be an important aspect for the study of Ag(I) or other metals on natural quartz sand.

### 3.2. Experimental procedure

The sorption experiments were carried out in batch reactors (polyethylene bottles, sand mass of 5 g, reactor volume of 50 mL, 298 K and no light for avoiding photoreaction of Ag). The range in initial concentration of Ag(I) was between  $5.0 \times 10^{-7}$  and  $1.0 \times 10^{-2}$  M. For each given concentration, three reactors containing liquid and solid phases, and a blank containing liquid phase only, were prepared for checking the reproducibility of experiments.

A stock solution of 0.10 M Ag(I) was prepared by weighing (Sartorius LA 3105, detection limit  $> 0.1$  mg)  $\text{AgNO}_3$  (99.8%, Prolabo 21 572.133), diluted in ultra pure water ( $18.2 \text{ M}\Omega \text{ cm}$ , Milli Q, Millipore). Different Ag(I) solutions were adjusted by successive dilutions from a stock solution. Before adding Ag(I) to a solution of  $\text{NaNO}_3$  (ionic strength: 0.010 M), the initial pH, pH<sub>i</sub>, was adjusted (WTW pH 330) by adding  $\text{HNO}_3$  (1.0 M) or  $\text{NaOH}$  (5.0 M). Solutions were buffered with MES (2 morpholinoethane sulfonic acid monohydrate) ( $2.0 \times 10^{-3}$  M) for pH<sub>i</sub> 6 and with HEPES (4 (2 hydroxyethyl) piperazine 1 ethane sulfonic acid) ( $2.0 \times 10^{-3}$  M) for pH<sub>i</sub> 8. When pH<sub>i</sub> was constant, the volume (50 mL) of  $\text{AgNO}_3$  was added in the reactor containing the sand.

The reactors were kept in the dark for 4 days (5760 min) and manually agitated twice a day for avoiding grinding of sand grains. The Ag sorbed on sand was calculated from concentration differences between initial and final aqueous concentrations of isotherm experiments and expressed in  $\text{mol m}^{-2}$  using the given specific surface area of each material.

### 3.3. Aqueous and surface analyses

After experiments, solid and liquid phases were separated for different analyses. Total silver, as  $^{107}\text{Ag}$  and  $^{109}\text{Ag}$  isotopes, were analyzed with an ICP MS (VG Plasma Quad3) or ICP AES (Elan 6000, Perkin Elmer) depending on Ag concentration. Anions were analyzed by anion chromatography ICS 2000 (DIONEX, column: Ion Pac AS11 Analytical ( $4 \times 250$  mm) Product No. 044076). This technique quantified the total concentration of fluorides, chlorides, bromides, nitrites, nitrates, phosphates and sulfates for a range of concentration between 1.0 and  $50 \text{ mg L}^{-1}$ . The pH of solution was also measured after experiments. For some experiments, Fe and Al were analyzed by ICP OES [30].

Qualitative analyses of rinsed sand were performed before and after experiments at pH<sub>i</sub> 6 with a Scanning Electron Microscope (Jeol 6360LV, at LMTG) equipped with an Energy Dispersive X ray Spectrometer (SEM EDS). XPS analyses were performed as described by Bonnissel Gissinger et al. [12].

## 4. Results

### 4.1. Ag(I) sorption on pure quartz sand

The Ag(I) sorption isotherm on pure quartz sand are reported for pH<sub>i</sub> 4 and 6, at 298 K in Fig. 1a. There was no change in the pH value during sorption on pure quartz sand. The adsorption capacities of pure quartz sand are very low and the amount of Ag sorbed are not measurable for  $[\text{Ag}]_i < 0.1 \mu\text{M}$ . Adsorption shows an asymptotic trend depending on initial pH at high concentration of Ag(I).

### 4.2. Ag(I) sorption on washed "natural" quartz sand

The Ag(I) sorption isotherms on washed natural quartz sand (treatment I) are displayed for 4 different pH<sub>i</sub> ( $\sim 2, 4, 6$  and 8) in Fig. 1b. Initial and final pH are reported in Table 1. There was no significant change of pH at pH<sub>i</sub> 2. At pH<sub>i</sub> 4 and 6, the pH increased while the pH decreased at pH<sub>i</sub> 8 after sorption of Ag(I). Increasing pH<sub>i</sub> resulted in the increase in Ag(I) adsorption capacities, except for pH<sub>i</sub>  $\sim 8$  and  $[\text{Ag}]_{\text{aq}} < 10^{-6}$  M. As observed, the washed natural quartz sand adsorbs more than the pure quartz sand. This could be explained by the presence of trace minerals which would play a very important role in the case of Ag(I) sorption.

Isotherms show a Langmuir type behavior for all pH with an asymptotic trend at high values of  $[\text{Ag}]_{\text{aq}}$ . At pH<sub>i</sub>  $\sim 4, 6$  and 8, the sorption isotherms of Ag(I) on the washed natural quartz sand have the same shape. For low Ag concentrations, the isotherms have a concave form, and for higher Ag concentrations, the isotherms become convex, except at pH<sub>i</sub>  $\sim 2$ .

### 4.3. Ag(I) sorption on rinsed "natural" quartz sand

Ag(I) sorption isotherm on rinsed natural quartz sand (treatment II) at pH<sub>i</sub>  $\sim 6$  for initial concentration ranges between  $1.0 \times 10^{-7}$  and  $1.0 \times 10^{-2}$  M was plotted together in Fig. 2a. Ag(I) isotherms were different for the two sands. During the experiment, the pH<sub>i</sub> was 6.12 and decreased to 5.7–5.9 after Ag(I) sorption. Aqueous anions were analyzed by ionic chromatography. Sulfate



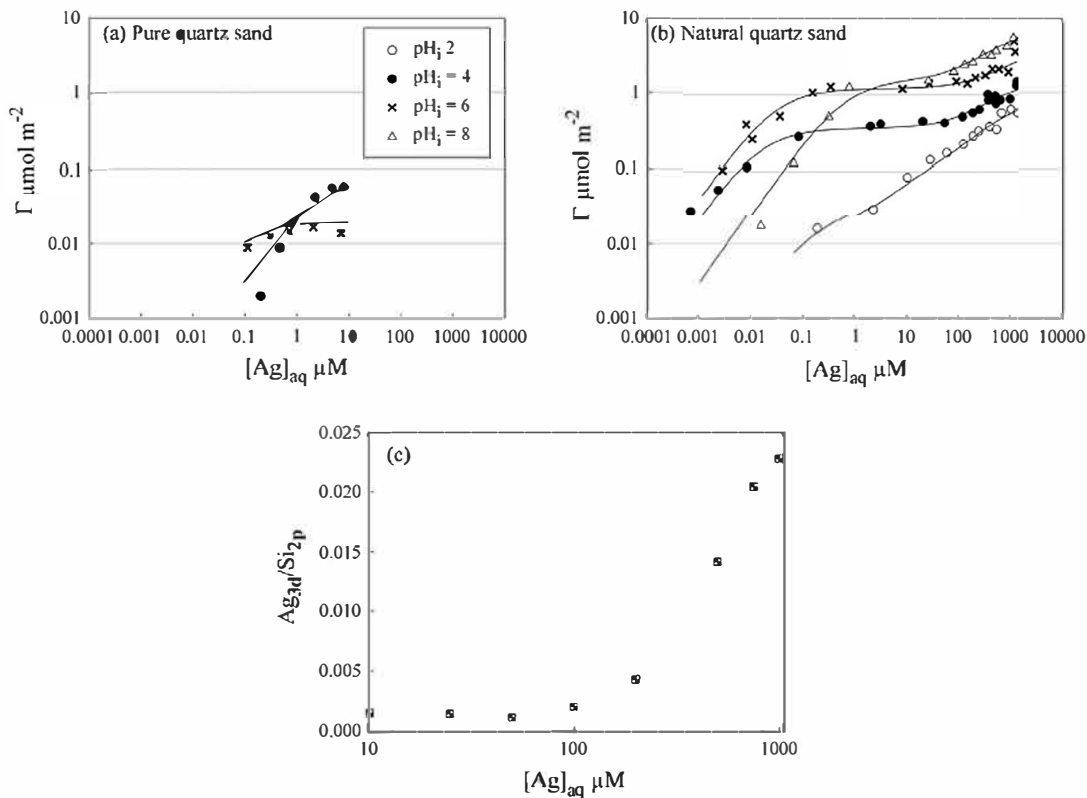


Fig. 1. Sorption Ag(I) isotherms according to pH<sub>i</sub> (a) on pure quartz sand, (b) on washed natural quartz sand (treatment I) with isotherms calculated by MICROQL (logarithmic scales) at 298 K, and (c) Ag(I) isotherm calculated from XPS analyses, showing Ag<sub>3d</sub>/Si<sub>2p</sub> atomic ratio on washed natural quartz sands (treatment I) vs total aqueous Ag, at pH<sub>i</sub> 4. For both sands, x-axis represents the total concentration of Ag(I) estimated by ICP-MS.

ions were detected at about  $2.6 \times 10^{-5}$  M. At the same time, column experiments with tributyltin have been performed [30]. Analyses of outlet column solutions have shown the presence not only of Fe and Al as Bianchi et al. [27] but also of S to the average concentration of which has been around  $1.7 \times 10^{-5}$  M, i.e. the same order of magnitude as in the batch reactors used in this study.

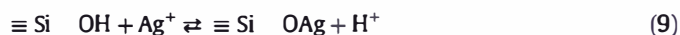
The rinsed sand was then analyzed after Ag(I) sorption by SEM EDS and XPS. Ag was not detectable directly on the silica except at high concentration. At pH 4 and Ag concentration higher than  $2.0 \times 10^{-5}$  M, Ag represents around 0.4 atomic percent of the sand surface. From SEM pictures, precipitates of metallic silver (Fig. S2a) and silver sulfide (Fig. S2e) were highlighted and confirmed by EDS spectrum (Fig. S2b and S2f). Clays were observed to have set Ag within their layers. The Fig. S2c depicts the smectite clay or chlorite surrounded by silica. The EDS spectrum (Fig. S2d) corresponding to this clay sample exhibits strong peaks correlating to Si, Al, O, Ag and weak peaks of Fe and Mg.

## 5. Discussion

### 5.1. Modeling of sorption data

#### 5.1.1. Pure quartz sand

For modeling sorption data on pure quartz sand, it was assumed that silica sites are the only available sites according to the following surface reactions



The  $\text{p}K_{\text{a}}$  values used for modeling are  $\text{p}K_{\text{a}1} = 0.95$  and  $\text{p}K_{\text{a}2} = 6.95$  for silica [31].

Estimated surface site concentrations and Langmuir type constants are reported in Table 1. Calculated isotherms show a good fit to the sorption data except at pH<sub>i</sub> 4 and  $[\text{Ag}]_{\text{aq}} < 0.5 \times 10^{-6}$  M (see Fig. 1). This confirmed the hypothesis that only one type of

Table 1  
Estimated parameters, for sorption isotherms of Ag(I) on pure quartz sand and washed natural quartz sand (treatment I), with Langmuir-type model at 1, 2 or 3 sorption sites.

pH <sub>i</sub>	pH <sub>eq</sub>	$\Gamma_{\text{max},1}$ $\mu\text{mol m}^{-2}$	$\text{Log } K_{\text{ads},1}$ $\text{M}^{-1}$	$\Gamma_{\text{max},2}$ $\mu\text{mol m}^{-2}$	$\text{Log } K_{\text{ads},2}$ $\text{M}^{-1}$	$\Gamma_{\text{max},3}$ $\mu\text{mol m}^{-2}$	$\text{Log } K_{\text{ads},3}$ $\text{M}^{-1}$
<i>Pure quartz sand</i>							
4.00	4.00	0.07	5.67	—	—	—	—
6.00	6.00	0.02	7.06	—	—	—	—
<i>Washed natural quartz sand</i>							
2.00–2.01	2.03–2.04	0.022	6.86	0.088	4.90	0.760	3.30
3.94–4.05	4.34–4.68	0.36	7.90	1.22	3.30	—	—
5.97–6.01 <sup>a</sup>	5.83–5.88	1.22	7.61	3.06	3.00	—	—
7.86–7.99 <sup>b</sup>	7.61–7.77	1.56	6.30	6.0	3.30	—	—

<sup>a</sup> [MES] = 2 mM.

<sup>b</sup> [HEPES] = 2 mM.

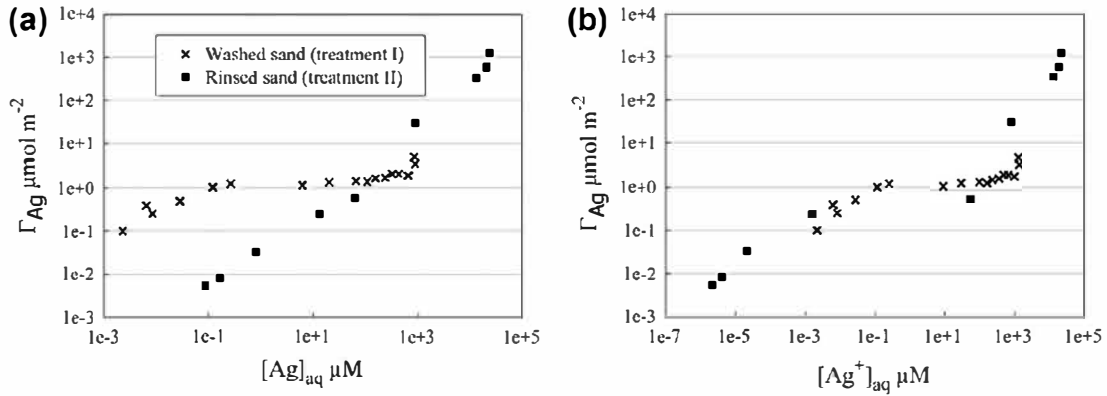


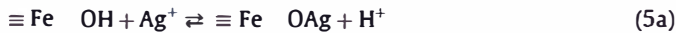
Fig. 2. Sorption Ag(I) isotherms on washed natural quartz sand (treatment I) and rinsed natural quartz sand (treatment II) at pH<sub>i</sub> 6 and 298 K: surface Ag(I) concentration vs. (a) total aqueous Ag(I) concentration as measured by ICP-MS or ICP-AES, and (b) calculated aqueous Ag<sup>+</sup> concentration by taking into account aqueous complexes (logarithmic scales).

surface sites is necessary for describing Ag(I) sorption on this sand. The values of sorption capacity,  $\Gamma_{max}$ , (Table 1) show that the surface site density of silica is very low. This result is in agreement with the work of Malati et al. [32] who have found an Ag(I) sorption capacity of  $0.03 \mu\text{mol m}^{-2}$  at pH 5 on precipitated silica, the specific surface area of which was however very high,  $149 \text{ m}^2 \text{ g}^{-1}$ . The surface complexation constants estimated from our data are very high (Table 1), what shows a strong affinity of Ag(I) to the pure quartz sand.

### 5.1.2. "Natural" quartz sand

According to natural quartz sand composition, the surface sites for metal cations could be silica, Fe, Al or Mn hydr(oxides), clays, and even pyrite. During treatment I applied to the sand, some pyrite and clays were probably dissolved and leached with the washing water. These minerals were not highlighted in the washed natural quartz sand by SEM EDS. Then, for modeling sorption data, it was assumed that iron (hydr)oxides were the primary surface sites and that silica acted as secondary surface sites (Eq. (9)). At pH<sub>i</sub> 2, a third site was necessary for optimizing the fitting with experimental data and assumed to be present on iron (hydr)oxides [33].

The postulated chemical reaction for Ag(I) reacting with iron (hydr)oxide surface sites is the same as used by Dzombak and Morel [8], i.e.:



The  $pK_a$  values for iron (hydr)oxides used for modeling are  $pK_{a1} = 6.60$  and  $pK_{a2} = 9.25$  [17].

From calculations, it was shown that two sorption sites were sufficient to describe the experimental data at pH<sub>i</sub> ~4, 6 and 8 whereas three sorption sites were necessary at pH<sub>i</sub> ~2 (Fig. 2b). For Ag(I) concentrations above  $600 \mu\text{M}$  and a high pH corresponding to a change in slope, both surface complexation and surface precipitation are assumed [8,33].

A good correlation exists between experimental data and modeling. However, estimated values of surface complexation constants were a function of pH (Fig. 3). Thus, the behavior of Ag(I) cannot be predicted for all experimental conditions with these values.

Moreover, for each site, the sorption capacity,  $\Gamma_{max,i}$  increased with increasing pH (Table 1). For example, the sorption capacity of the first site is  $0.022 \mu\text{mol m}^{-2}$  for pH<sub>i</sub> ~2 and  $1.56 \mu\text{mol m}^{-2}$  for pH<sub>i</sub> ~8. This suggests that sand washed with water in a column behaves like a cation exchanger for weak acids [16]. The pH variations due to Ag(I) sorption are listed in Table 1. The pH variation

with the washed quartz sand was detected while the pH change for pure quartz sand was not measurable. The measurable variation of pH with natural sands can be due to two mechanisms at least: (i) dissolution of minerals present at the surface of the "natural" sands and (ii) the exchange between H<sup>+</sup> and Ag<sup>+</sup> during sorption at the surface sites. At pH<sub>i</sub> < 6, the increase in pH after Ag(I) sorption could be due to the dissolution of metallic (hydr)oxides (Fe, Al and Mn), reactions which need H<sup>+</sup> ions. This is consistent with the results of both Bianchi et al. [27] who have found aqueous Fe and Al after agitating this sand during 1 h at pH 4, and Rafidariison [30]. At pH<sub>i</sub> 8, the pH decreased after Ag(I) sorption. In basic medium, dissolution of metallic (hydr)oxides always occurs in addition to the dissolution of some pyrite remaining after treatment I.

### 5.2. Influence of sand treatment on Ag(I) speciation

Due to mineral dissolution, the Ag(I) speciation could be different during the sorption on the two "natural" sands. The experimental conditions were the same except the washing treatment before sorption experiments. As shown by Bianchi et al. [27] and Bueno et al. [25], the treatment applied to the sand may change its surface reactivity. With respect to Ag(I), this change would imply different possible interactions with sand surface. The possible minerals of the sand, which can dissolve during treatment con

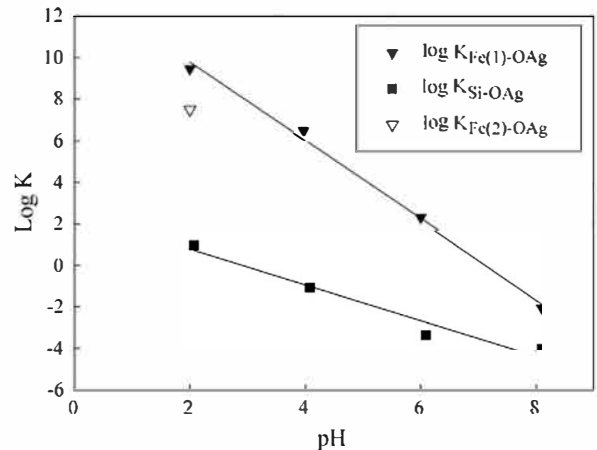


Fig. 3. Conditional surface complexation constants of Ag(I) vs. pH in presence of washed natural quartz sand (treatment I) for the different sites, at 298 K. Linear regression:  $\log K_{Fe(1)-OAg} = -1.88 \text{ pH} + 13.55$ ,  $R = 0.9974$ ;  $\log K_{Si-OAg} = -0.85 \text{ pH} + 2.76$ ,  $R = 0.9792$ .

ditions, are Al, Fe and Mn (hydr)oxides along with pyrite. The presence of sulfates in the reactor after experiments can be due to pyrite dissolution because the only other mineral containing sulfates was the barite which was assumed insoluble in studied conditions. Another fact in favor of pyrite dissolution was the characterization of metallic silver (Fig. S2a and S2b) and silver sulfur precipitate by SEM EDS (Fig. S2e and S2f). This is consistent with the analyses and explanations of Scaini et al. [6] and Eq. (4) showing that redox reaction occurring at the surface of pyrite between sulfur and Ag(I) leads to both the reduction of Ag(I) to Ag(0) and of S( I) to S( II) followed by precipitation of Ag<sub>2</sub>S, and the oxidation of S( I) to S(VI). The presence of SO<sub>4</sub><sup>2-</sup> in aqueous solution could have been provided by the interaction of Ag(I) with pyrite. According to the mechanism proposed by Eq. (4) [6], the formed species in solution are SO<sub>4</sub><sup>2-</sup>, Fe<sup>2+</sup> and H<sup>+</sup>. It has been reported that at pH 6, the oxidation of Fe(II) to Fe(III) in pyrite is fast and that the precipitation of Fe(III) (hydr)oxides is possible [12]. The surface of pyrite is then more heterogeneous and consists of Fe(II) and Fe(III) (hydr)oxides. When protons are combined the pH dropped rapidly to 4 from an initial pH between 5 and 10. At pH<sub>i</sub> 4, pyrite is highly reactive and unstable due to its high oxidizing capacity and is oxidized to Fe(III) and SO<sub>4</sub><sup>2-</sup>.

The concentration of the sulfur compound most oxidized, SO<sub>4</sub><sup>2-</sup>, is about  $2.6 \times 10^{-5}$  M but prior to anion chromatography measurements, sulfur had to be in other forms like sulfites, sulfides and/or thiosulfates during oxidative dissolution of pyrite [12,34]. The presence of these sulfur compounds can strongly change the aqueous Ag(I) speciation. Indeed Ag(I) can form more or less stable complexes with sulfur species such as SO<sub>4</sub><sup>2-</sup>, S<sup>2-</sup>, SO<sub>3</sub><sup>2-</sup> and S<sub>2</sub>O<sub>3</sub><sup>2-</sup> (see list of stability constants in Table S2) [35].

According to Eqs. S30 to S34, Ag(I) forms three different complexes with S<sub>2</sub>O<sub>3</sub><sup>2-</sup> depending on physical chemical composition of aqueous solutions. The formation of such aqueous Ag(I) complexes strongly decreases the free aqueous Ag<sup>+</sup> resulting in a decrease in the possible interactions with surface sites. Assuming that the initial concentration of S<sub>2</sub>O<sub>3</sub><sup>2-</sup> is about  $2.6 \times 10^{-5}$  M, free Ag(I) concentration was calculated for each experiment. The data of Ag(I) sorption were then plotted vs. the free Ag(I) concentration calculated by taking into account S<sub>2</sub>O<sub>3</sub><sup>2-</sup> concentration. In this case, both data sets of Ag(I) sorption at pH 6 were superimposed. Results were similar if complexes between Ag(I) and S( II) was assumed in the system. However no effect was highlighted by taking into account aqueous complexation of Ag(I) with SO<sub>3</sub><sup>2-</sup> or SO<sub>4</sub><sup>2-</sup>. According to these results, it appears that the change in mineral composition of the surface of "natural" quartz sands due to its aging during treatment plays an important role in surface reactivity and interactions. During the treatment I (20 days), a large part of pyrite was dissolved and the dissolved products were exported to the outlet of the column and then lost. In contrary, after the treatment II, minerals stayed in studied system and then played an important role in the Ag(I) speciation. This point is very important in the case of aquifer which evolves slowly with time, e.g. in the case of nuclear waste disposal. Indeed, the dissolution of some minerals can be significant with percolating water and change readily the speciation of heavy metals such as Ag and thus their fate in the nearby environment.

So far, it was assumed that the surface sites of iron (hydr)oxides and silica were the main actors for controlling the surface complexation. Indeed, the role of clays was minimized. The clays mainly present as kaolinite, illite and smectite (0.1% of the total mass of sand) could be considered as potential adsorbents of cations. Behra [23] have observed on the same type of natural material that the sorption of Hg(II) on clays is about  $0.8 \mu\text{mol g}^{-1}$  of total sand. The Hg(II) sorption on silica and iron (hydr)oxides was about  $0.5 \text{ nmol g}^{-1}$  and  $5.4 \mu\text{mol g}^{-1}$ , respectively. The clays

present in the "natural" sand can thus play a more important role than silica in the sorption of Hg(II) even if the clays are present in small proportion. With respect to the Ag(I), the SEM EDS analysis (see Fig. S2c and S2d) show that interactions between clays and Ag would occur which is consistent with the works of Jacobson et al. [9]. In our case, modeling with silica and iron hydro(oxides) was sufficient but it would be interesting to study materials containing a larger proportion of clays.

### 5.3. Effect of HEPES at basic pH

In literature, HEPES have been using for many chemical and biological studies because of its known neutrality towards the metal ions [36,37]. However, the study of Vasconcelos et al. [38] have shown that HEPES was able to bind Cu(II) when HEPES was in large excess ( $2000 < \text{HEPES}/\text{Cu} < 10000$ ) at pH 8. They have reported that the importance of complexation was even more pronounced when the Cu concentration was low. HEPES represents a weak zwitter ionic acid at low pH with low affinity for cation. Although for high pH, the affinity between HEPES and cations increases due to the deprotonation of the acid [39]. According to these studies and stability constant estimation for Cu(II) by Mash et al. [40], a complexation reaction between HEPES and Ag(I) could thus explain the low Ag(I) sorption at pH<sub>i</sub> ~8 and for [Ag]<sub>aq</sub> < 1.0 μM (Fig. 1b).

### 5.4. Some input for environmental applications

From this study, it was shown the role of the surface composition of sand in the behavior of a trace metal such as Ag. Depending on local environmental conditions, Ag can react and be either sorbed as a surface complex on different minerals such as iron (hydr)oxides, silica and clays, or precipitated due to the presence of traces of pyrite and its redox dissolution. In the latter case, the implications may be important with respect to environmental systems: first some S<sub>2</sub>O<sub>3</sub><sup>2-</sup> or S( II) which are formed may dramatically change the Ag speciation, by increasing aqueous Ag concentration and in turn Ag mobility; and secondly some Ag(0) colloids, the mobility of which has to be investigated at larger scale to evaluate their possible migration, can be formed at the surface of sand grains. Ag is an interesting probe since its reactivity depends strongly on redox conditions. Other metals which are present in waste such as nuclear waste are also strongly redox dependent. Thus, it is obviously shown in this study how traces of pyrite which control redox conditions have to be taken into account for avoiding great mistakes in modeling transport at large scale.

## 6. Conclusions

The main objective of this study was to better understand the behavior of Ag(I) in the presence of a natural sand mainly composed of quartz but having some natural impurities such as clays, traces of iron (hydro)oxides and pyrite. Sorption results were compared to a pure quartz sand in order to clearly identify the different Ag(I) adsorption sites. The sorbed Ag concentration is strongly dependent on pH with isotherms characterized by superimposition of Langmuir type isotherms for initial Ag(I) concentration range between  $0.5 \times 10^{-6}$  and  $1.0 \times 10^{-3}$  M. From experimental data fitting taking into account speciation calculation, several sites are proposed.

At pH<sub>i</sub> 4, 6 and 8, the first surface site is assumed to be due to iron (hydr)oxides while the second surface site is attributed to silanols. At pH<sub>i</sub> 2, sorption of Ag(I) would take place on two surface sites of iron (hydr)oxides and a third surface site on silanol groups. Moreover the presence of pyrite, which was highlighted by aqueous sulfates due its redox dissolution, is assumed to control part



of Ag behavior, as shown by Scaini et al. [6]. In such heterogeneous and natural system, iron (hydr)oxides, sulfates, and sulfur compounds can react with Ag(I) and in turn control its reactivity both in the aqueous phase and at the solid liquid interface. The possible reactions with ligands such as thiosulfates can explain the fate of Ag(I) sorption when pyrite is still present, even at a low level. SEM EDS analyses proved the assumption of precipitation of Ag sulfur species and surface precipitation of metallic Ag, for high initial concentrations of Ag(I) ( $>10^{-3}$  M). On the other hand, XPS chemical surface analysis confirmed shape of complex sorption isotherm from the point of view of the solid surface.

Consequently, we showed that all the minerals, even those present at low surface concentration, can control the transfer of trace compounds. The main issue is that it is absolutely necessary to get the best knowledge of their speciation and sorption mechanisms at atomic scale for reactive transport modeling at larger scale, e.g. for waste disposals such as radioactive nuclear compounds.

For improving the knowledge of the Ag(I) behavior in the environment, further research would be necessary to quantify the influence of the pyrite dissolution kinetics [13,14] and look more closely at the contribution of other minerals such as clays in the Ag(I) sorption in a large scale transport modeling.

## Acknowledgments

We thank T. Aigouy (Géosciences Environnement Toulouse (GET), Université Paul Sabatier, CNRS, IRD, OMP, Toulouse, France) for the SEM images, M. Bueno (IPREM/LCABIE, Pau, France) for the ICP AES analysis, the GET for ICP MS analysis, J. Lambert and J.J. Ehrhardt (LCPME, CNRS, Nancy) for XPS analyses, and H. Rafidiarison. The major part of experiments was performed at the IMF Strasbourg. MAHC was supported by a grant from SEP CONACYT IPN.

## Appendix A. Supplementary material

Supplementary data associated with this article can be found, in the online version, at <http://dx.doi.org/10.1016/j.jcis.2014.12.050>.

## References

- [1] B. Nowack, H. Krug, M. Height, *Environ. Sci. Technol.* 45 (2011) 1177–1183.
- [2] E. Navarro, F. Piccapietra, B. Wagner, F. Marconi, R. Kaegi, N. Odzak, L. Sigg, R. Behra, *Environ. Sci. Technol.* 42 (2008) 8959–8964.
- [3] S. Egger, R.P. Lehmann, M.J. Height, M.J. Loessner, M. Schuppler, *Appl. Environ. Microbiol.* 75 (2009) 2973–2976.
- [4] A. Teruo, S. Satoshi, G. Hiroshi, N. Masanori, K. Masatsugu, *Nutrition* 71 (2000) 179–186.
- [5] D. He, J.J. Dorantes-Aranda, T.D. Waite, *Environ. Sci. Technol.* 46 (2012) 8731–8738.
- [6] M.J. Scaini, G.M. Bancroft, J.W. Lorimer, L.M. Maddox, *Geochim. Cosmochim. Acta* 59 (1995) 2733–2747.
- [7] R. Ravikumar, D.W. Fuerstenau, *Silver sorption by manganese oxide*, in: J.A. Voigt, T.E. Wood, B.C. Bunker, W.H. Casey, L.J. Crosse (Eds.), *Materials Research Society Symposium Proceedings: Aqueous Chemistry and Geochemistry of Oxide, Oxyhydroxides and Related Materials* 432, Materials Research Society, Warrendale, PA, 1997, pp. 243–248.
- [8] D.A. Dzombak, F.M.M. Morel, *Surface Complexation Modeling: Hydrous Ferric Oxide*, John Wiley & Sons, New York, 1990.
- [9] A.R. Jacobson, M.B. McBride, P. Baveye, T.S. Steenhuis, *Sci. Total Environ.* 345 (2005) 191–205.
- [10] P. Behra, P. Bonnissel-Gissing, M. Alnot, R. Revel, J.J. Ehrhardt, *Langmuir* 17 (2001) 3970–3979.
- [11] R.T. Lowson, *Chem. Rev.* 82 (1982) 461–497.
- [12] P. Bonnissel-Gissing, M. Alnot, J.J. Ehrhardt, P. Behra, *Environ. Sci. Technol.* 32 (1998) 2839–2845.
- [13] M.A. Williamson, J.D. Rimstidt, *Geochim. Cosmochim. Acta* 58 (1994) 5443–5454.
- [14] A. Gartman, G.W. III Luther, *Geochim. Cosmochim. Acta* (2014).
- [15] I. Langmuir, *J. Am. Chem. Soc.* 40 (1918) 1361–1403.
- [16] W. Stumm, J.J. Morgan, *Aquatic Chemistry: Chemical Equilibria and Rates in Natural Waters*, third ed., John Wiley & Sons, New York, 1996.
- [17] L. Sigg, P. Behra, W. Stumm, *Chimie des milieux aquatiques*, fifth ed., Dunod, Paris, 2014.
- [18] J.C. Westall, MICROQL-II. Computation of adsorption equilibria in BASIC. Technical report, EAWAG, Dübendorf, Switzerland, 1979.
- [19] J.C. Westall, MICROQL-I. A chemical equilibrium program in BASIC, Version 2 for PC's. Technical Report 86-02, Oregon State University, Corvallis, Oregon, 1986.
- [20] F.M.M. Morel, *Principles of Aquatic Chemistry*, Wiley, New York, 1983.
- [21] M. Bueno, A. Astruc, M. Astruc, P. Behra, *Environ. Sci. Technol.* 32 (1998) 3919–3925.
- [22] M. Hernández Cortázar, *Etude cinétique et thermodynamique de la sorption de l'argent (I) sur des sables de quartz*. Ph.D. Dissertation, Université Louis Pasteur, Strasbourg, 2003.
- [23] P. Behra, *Etude du comportement d'un micropolluant métallique – le mercure – au cours de sa migration à travers un milieu poreux saturé: identification expérimentale des mécanismes d'échanges et modélisation des phénomènes*. Ph.D. Dissertation, Université Louis Pasteur, Strasbourg, 1987.
- [24] P. Behra, *Geoderma* 38 (1986) 209–222.
- [25] M. Bueno, A. Astruc, J. Lambert, M. Astruc, P. Behra, *Environ. Sci. Technol.* 35 (2001) 1411–1419.
- [26] P. Behra, E. Lecarme-Théobald, M. Bueno, J.J. Ehrhardt, *J. Colloid Interface Sci.* 263 (2003) 4–12.
- [27] A. Bianchi, M. Petrangelo, *Water Sci. Technol.* 48 (2004) 9–16.
- [28] V. Trommetter, *Contribution à l'étude du transport d'arséniate à travers un milieu poreux d'origine naturelle*. Ph.D. Dissertation, Université Louis Pasteur, Strasbourg, 1999.
- [29] M.A. Hernandez Cortazar, P. Behra, *J. Phys. IV France* 107 (2003) 609–612.
- [30] H.M. Rafidiarison, *Influence de la dissolution des minéraux d'un sable naturel de quartz sur le comportement du tributylétain à de très faibles concentrations*. Master Dissertation, Institut National Polytechnique and Université Paul Sabatier, Toulouse, 2005.
- [31] C. Tiffreau, J. Lützenkirchen, P. Behra, *J. Colloid Interface Sci.* 172 (1995) 82–93.
- [32] M.A. Malati, M. McEvoy, C.R. Harvey, *Surface Technol.* 17 (1982) 165–174.
- [33] K.J. Farley, D.A. Dzombak, F.M.M. Morel, *J. Colloid Interface Sci.* 106 (1985) 226–242.
- [34] M. Descostes, P. Vitorge, C. Beaucaire, *Geochim. Cosmochim. Acta* 68 (2004) 4559–4569.
- [35] A.E. Martell, R.M. Smith, R.J. Motekaitis, *NIST critical stability constant of metal complexes database [NIST standard reference database 46]*, U.S. Department of Commerce, Gaithersburg, MD, 1988.
- [36] N.E. Good, S. Izawa, *Methods Enzymol* 24 (1972) 53–68.
- [37] N.E. Good, G.D. Winget, W. Winter, T.N. Connolly, S. Izawa, R.M.M. Singh, *Biochemistry* 5 (1966) 467–477.
- [38] M.T.S.D. Vasconcelos, M.A.G.O. Azenha, O.M. Lage, *Anal. Biochem.* 241 (1996) 248–253.
- [39] J.E. Mclean, B.E. Bledsoe, *Ground water issue: behavior of metals in soils*. US Environmental Protection Agency, EPA/540/S-92/018, 1992, pp. 1–25.
- [40] H.E. Mash, Y.P. Chin, L. Sigg, R. Hari, H. Xue, H. Anal, *Chemistry* 75 (2003) 671–677.

## Supplementary material for:

# Effect of the presence of pyrite traces on silver behavior in natural porous media

*Delphine Charrière<sup>1,2</sup>, Manuel de A. Hernández Cortàzar<sup>3</sup>, Philippe Behra<sup>1,2,\*</sup>*

1. Université de Toulouse; INPT, LCA (Laboratoire de Chimie AgroIndustrielle); ENSIACET, 4, Allée

Emile Monso, BP44362, F-31030 Toulouse Cedex

2. INRA; LCA (Laboratoire de Chimie AgroIndustrielle); F-31030 Toulouse

3. CMPL (Centro Mexicano Para la Producción más Limpia), Instituto Politecnico Nacional, Av. IPN s/n, Unidad Profesional Adolfo López Mateos, Laboratorio Pesado E.S.F.M., Zacatenco, 07738 Mexico,

D.F., México

Corresponding author. E-mail: [philippe.behra@ensiacet.fr](mailto:philippe.behra@ensiacet.fr).

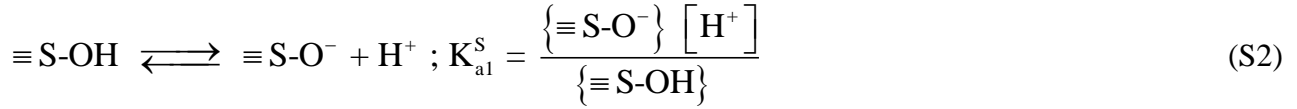
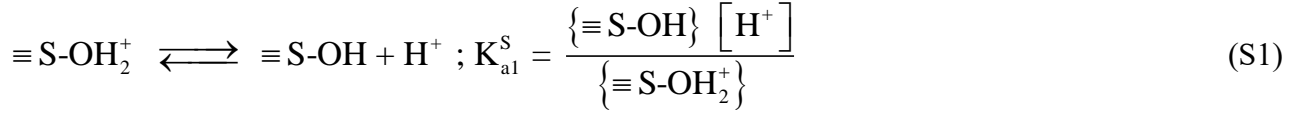
† Université de Toulouse.

‡ INRA.

§ CMPL.

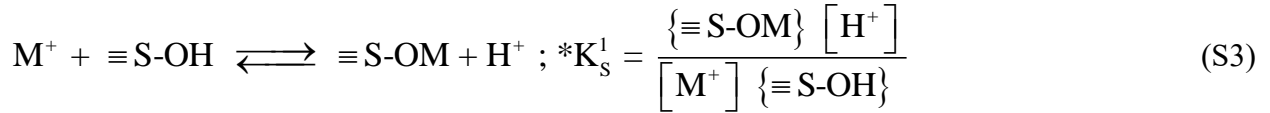
SI includes two figures and two tables in six pages

**Surface acidity and surface complexation.** The functional groups (-OH, -COOH, -NH<sub>2</sub>, -SH) of solid surface become weak acids or bases according to the pH and can be represented by two reactions with two pK<sub>a</sub>:



where  $\{\equiv\text{S-OH}\}$  is the concentration of surface sites (mol m<sup>-2</sup>),  $K_{a1}^S$  and  $K_{a2}^S$  are the apparent constants of acidity.

The surface complexation occurs when a metal cation reacts with an anion which functions as an organic ligand and forms covalent bonds (10). Surface sites are ligands against to metal cations M<sup>+</sup>, forming a monodentate complex  $\equiv\text{S-OM}$ :



where  $*K_s^1$  is the equilibrium constant.

The total surface sites are:

$$S_{\text{max}} = \{\equiv\text{S-OH}_2^+\} + \{\equiv\text{S-OH}\} + \{\equiv\text{S-O}^-\} + \{\equiv\text{S-OM}\} \quad (\text{S4})$$

When eqs S1 and S2 are substituted in eq S4, the equation becomes:

$$S_{\text{max}} = \{\equiv\text{S-OH}\} \left( \frac{[\text{H}^+]}{K_{a1}^S} + 1 + \frac{K_{a2}^S}{[\text{H}^+]} \right) + \{\equiv\text{S-OM}\} \quad (\text{S5})$$

$$\text{And if it is assumed that: } \alpha_1 = \left( \frac{[\text{H}^+]}{K_{a1}^S} + 1 + \frac{K_{a2}^S}{[\text{H}^+]} \right)^{-1} \quad (\text{S6})$$

Then having  $\{\equiv\text{S-OH}\}$  from eq S3 and eq S5,  $S_{\text{max}}$  will be obtained as follows:

$$S_{\max} = \frac{\{\equiv\text{S-OM}\} [\text{H}^+]}{*K_1^{\text{S}} [\text{M}^+] \alpha_1} + \{\equiv\text{S-OM}\} \quad (\text{S7})$$

After factorization, eq S7 becomes:

$$\{\equiv\text{S-OM}\} = S_{\max} \frac{*K_1^{\text{S}} \alpha_1 [\text{H}^+]^{-1} [\text{M}^+]}{1 + *K_1^{\text{S}} \alpha_1 [\text{H}^+]^{-1} [\text{M}^+]} \quad (\text{S8})$$

**Aqueous solution/speciation.** In the case of a free ligand L complex with  $\text{M}^+$ , the speciation of  $\text{M}^+$  changes (10):



The total concentration of  $[\text{M}]_{\text{aq}}$  is:

$$[\text{M}]_{\text{aq}} = [\text{M}^+] + [\text{ML}^+] = [\text{M}^+] (1 + K_{\text{ML}} [\text{L}]) = [\text{M}^+] \alpha^{-1} \quad (\text{S11})$$

Then, eq (S8) can be expressed as:

$$\{\equiv\text{S-OM}\} = S_{\max} \frac{*K_1^{\text{S}} \alpha \alpha_1 [\text{H}^+]^{-1} [\text{M}]_{\text{aq}}}{1 + *K_1^{\text{S}} \alpha \alpha_1 [\text{H}^+]^{-1} [\text{M}]_{\text{aq}}} \quad (\text{S12})$$

If it is assumed that:

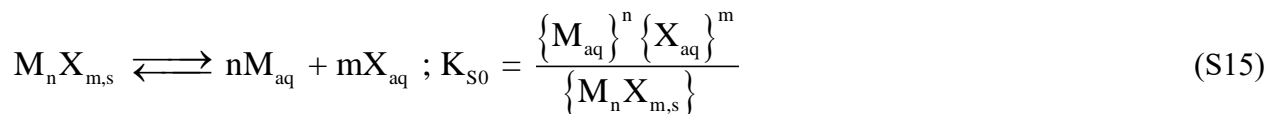
$$K_{\equiv\text{S-OM}} = *K_1^{\text{S}} \alpha \alpha_1 [\text{H}^+]^{-1} \quad (\text{S13})$$

Finally, eq (S14) can be obtained:

$$\{\equiv\text{S-OM}\} = S_{\max} \frac{K_{\equiv\text{S-OM}} [\text{M}]_{\text{aq}}}{1 + K_{\equiv\text{S-OM}} [\text{M}]_{\text{aq}}} \quad (\text{S14})$$

The relationship between  $\{\equiv\text{S-OM}\}$  and  $[\text{M}]_{\text{aq}}$  is Langmuir-type like, for the formation of a monodentate complex. Here, the electrostatic correction term is not taken into account.

**Solubility product.** A solubility equilibrium exists when a chemical compound in the solid state is in chemical equilibrium with a solution of that compound. For example, solubility equilibrium of solid phase,  $M_nX_{m,s}$ , can be expressed as:



If the solid phase is pure, its activity is fixed to equal 1. The constant  $K_{s0}$ , called solubility product, is simplified as follows:

$$K_{s0} = \{M_{aq}\}^n \{X_{aq}\}^m \quad (S16)$$

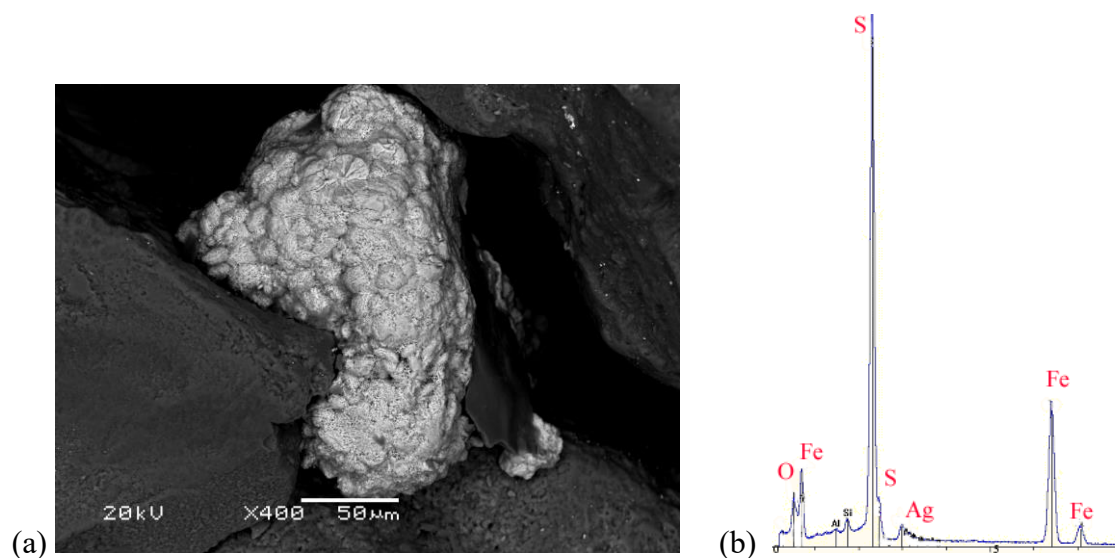


FIGURE S1. (a) SEM image (BEC) of pyrite in globular masses interspersed in the sand, (b) EDS spectrum of the pyrite (pH<sub>i</sub> 6, equilibrium time 5760 min, ionic strength 0.010 M (NaNO<sub>3</sub>), 5 g of sand (treatment II), [Ag<sup>+</sup>] = 10<sup>-2</sup> M, volume of solution 50 mL)



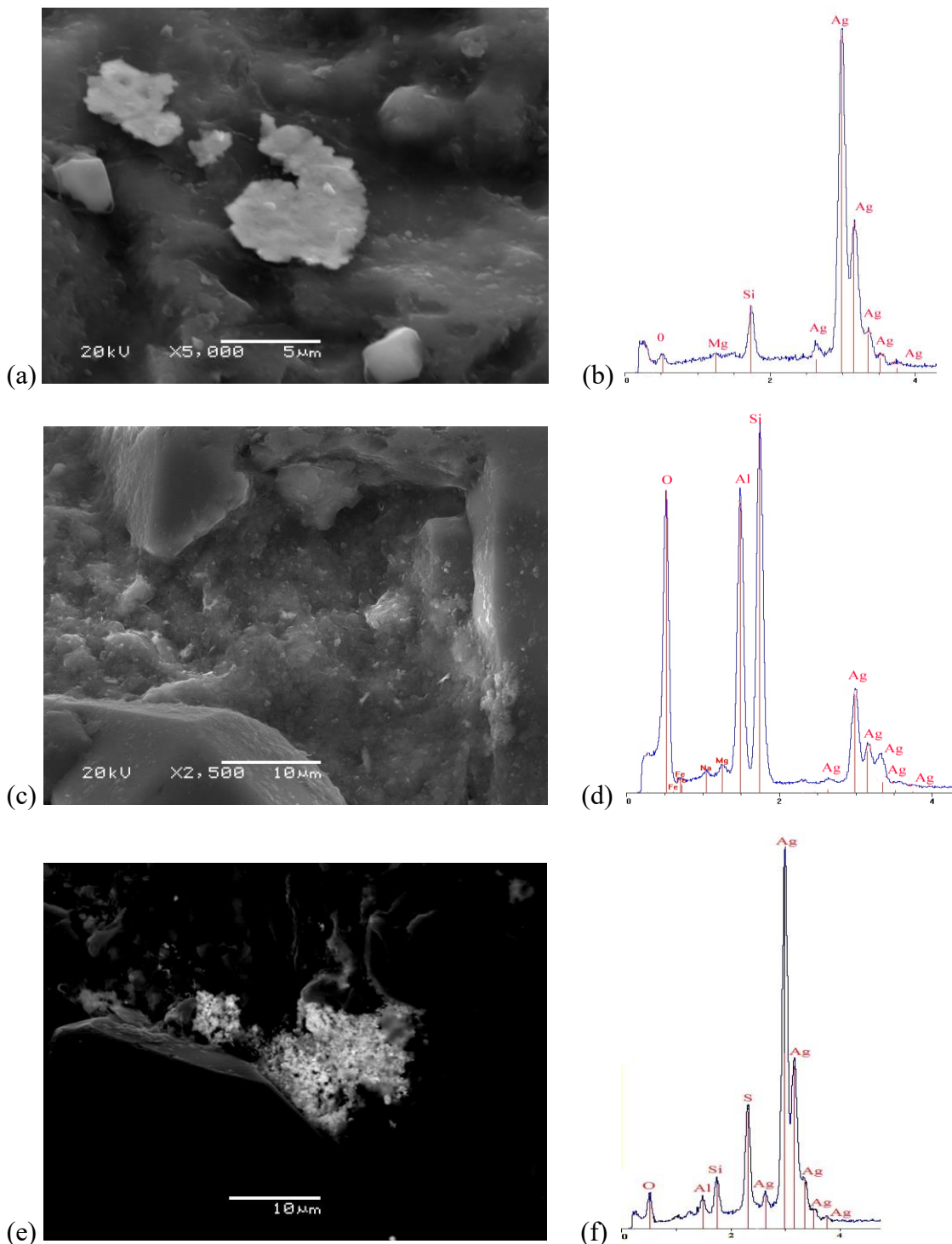


FIGURE S2. (a) SEM image (SEI) of a precipitate of metallic silver on the unwashed sand after Ag(I) sorption, (b) EDS spectrum corresponding to the precipitate, (c) SEM image (SEI) of a clay containing Ag(I) surrounded by silica of washed sand, (d) EDS spectrum taken from the clay, (e) SEM image (SEI) of a precipitate of  $\text{Ag}_2\text{S}$  on the washed sand and (f) EDS spectrum taken from  $\text{Ag}_2\text{S}$  precipitate ( $\text{pH}_i$  6, equilibrium time 5760 min, ionic strength 0.010 M ( $\text{NaNO}_3$ ), 5 g of sand (treatment II),  $[\text{Ag}^+] = 10^{-2}$  M, volume of solution 50 mL)

TABLE S1. Tableau summarizing data for Ag(I) speciation calculation (at 298.15 K)

		$\equiv\text{S-OH}$	$\text{L}^*$	$\text{Ag}^+$	$\text{H}^+$	$\log K$
1	Species: $\text{Ag}^+$			1		0
2	$\equiv\text{S-OH}_2^+$	1			1	$\log K_{\text{S-OH}_2^+}$
3	$\equiv\text{S-OH}$	1				$\log K_{\text{S-OH}}$
4	$\equiv\text{S-O}^-$	1			-1	$\log K_{\text{S-O}^-}$
5	$\equiv\text{S-OAg}$	1		1	-1	$\log K_{\text{S-OAg}}$
6	$\text{Ag-L}$		1	1		$\log K_{\text{Ag-L}}$
7	$\text{H-L}$		1		1	$\log K_{\text{H-L}}$
8	$\text{L}$		1			0
9	$\text{OH}^-$				-1	-14.00
10	$\text{H}^+$				1	0
Mass balance:		$[\equiv\text{S-OH}]_{\text{tot}}$	$[\text{L}]_{\text{tot}}$	$[\text{Ag}^+]_{\text{tot}}$	Fixed pH	

\* L represents ligands such as halides, sulfur anions, etc.

TABLE S2. Ag(I) complexes with sulfur species [35]

Ligands	Reactions of Ag <sup>+</sup> with ligands and H <sup>+</sup>		
SO <sub>4</sub> <sup>2-</sup>	Ag <sup>+</sup> + SO <sub>4</sub> <sup>2-</sup> ⇌ AgSO <sub>4</sub>	β <sub>1</sub> = 1.99	(S17)
	H <sup>+</sup> + SO <sub>4</sub> <sup>2-</sup> ⇌ HSO <sub>4</sub> <sup>-</sup>	β <sub>2</sub> = 1.3	(S18)
S <sup>2-</sup>	Ag <sup>+</sup> + S <sup>2-</sup> ⇌ AgS <sup>-</sup>	β <sub>2</sub> = 19.2	(S19)
	Ag <sup>+</sup> + H <sup>+</sup> + S <sup>2-</sup> ⇌ AgHS	β <sub>3</sub> = 27.7	(S20)
	Ag <sup>+</sup> + H <sup>+</sup> + 2S <sup>2-</sup> ⇌ AgHS <sub>2</sub> <sup>2-</sup>	β <sub>4</sub> = 35.8	(S21)
	Ag <sup>+</sup> + 2H <sup>+</sup> + 2S <sup>2-</sup> ⇌ AgH <sub>2</sub> S <sub>2</sub> <sup>-</sup>	β <sub>5</sub> = 45.7	(S22)
	H <sup>+</sup> + S <sup>2-</sup> ⇌ HS <sup>-</sup>	K <sub>2</sub> = 13.9	(S23)
	2H <sup>+</sup> + S <sup>2-</sup> ⇌ H <sub>2</sub> S	K <sub>3</sub> = 20.9	(S24)
SO <sub>3</sub> <sup>2-</sup>	Ag <sup>+</sup> + SO <sub>3</sub> <sup>2-</sup> ⇌ AgSO <sub>3</sub> <sup>-</sup>	β <sub>6</sub> = 5.6	(S25)
	Ag <sup>+</sup> + 2SO <sub>3</sub> <sup>2-</sup> ⇌ Ag(SO <sub>3</sub> ) <sub>2</sub> <sup>3-</sup>	β <sub>7</sub> = 8.7	(S26)
	Ag <sup>+</sup> + 3SO <sub>3</sub> <sup>2-</sup> ⇌ Ag(SO <sub>3</sub> ) <sub>3</sub> <sup>5-</sup>	β <sub>8</sub> = 9.0	(S27)
	H <sup>+</sup> + SO <sub>3</sub> <sup>2-</sup> ⇌ HSO <sub>3</sub> <sup>-</sup>	K <sub>4</sub> = 1.80	(S28)
	2H <sup>+</sup> + SO <sub>3</sub> <sup>2-</sup> ⇌ H <sub>2</sub> SO <sub>3</sub>	K <sub>5</sub> = 8.95	(S29)
S <sub>2</sub> O <sub>3</sub> <sup>2-</sup>	Ag <sup>+</sup> + S <sub>2</sub> O <sub>3</sub> <sup>2-</sup> ⇌ AgS <sub>2</sub> O <sub>3</sub> <sup>-</sup>	β <sub>9</sub> = 8.82	(S30)
	Ag <sup>+</sup> + 2S <sub>2</sub> O <sub>3</sub> <sup>2-</sup> ⇌ Ag(S <sub>2</sub> O <sub>3</sub> ) <sub>2</sub> <sup>3-</sup>	β <sub>10</sub> = 13.50	(S31)
	Ag <sup>+</sup> + 3S <sub>2</sub> O <sub>3</sub> <sup>2-</sup> ⇌ Ag(S <sub>2</sub> O <sub>3</sub> ) <sub>3</sub> <sup>5-</sup>	β <sub>11</sub> = 14.00	(S32)
	H <sup>+</sup> + S <sub>2</sub> O <sub>3</sub> <sup>2-</sup> ⇌ HS <sub>2</sub> O <sub>3</sub> <sup>-</sup>	K <sub>6</sub> = 0.60	(S33)
	2H <sup>+</sup> + S <sub>2</sub> O <sub>3</sub> <sup>2-</sup> ⇌ H <sub>2</sub> S <sub>2</sub> O <sub>3</sub>	K <sub>7</sub> = 2.30	(S34)

Where the β<sub>i</sub> and K<sub>i</sub> represent the global stability constant between the ligand and Ag<sup>+</sup>, and between the ligand and H<sup>+</sup>, respectively.